LAPP-EXP-94.25
DECEMBER 1994

PROGRESS IN $PbWO_4$ SCINTILLATING CRYSTAL

A. Fyodorov, M. Korzhik, O. Missevitch, V. Pavlenko
INP, Minsk, Belarus
V. Kachanov, A. Singovsky
IHEP, Protvino, Russia
A.N. Annenkov, V.A. Ligun
Spectr Co, Research Div., Tula, Russia
J.P. Peigneux, J.P. Vialle
LAPP, Annecy, France
J.L. Faure DAPNIA, CEA, Saclay, France
F. Binon, IISN Bruxelles, Belgique

Submitted to Radiation Measurements

L.A.P.P. B.P. 110 F-74941 ANNECY-LE-VIEUX CEDEX • TÉLÉPHONE 50.09.16.00+ • TÉLÉCOPIE 50 27 94 95

1. INTRODUCTION

Lead tungstate $PbWO_4$ (PWO) has recently been shown (V.G. Baryshevsky et al., 1992; M. Kobayashi, M. Ishii, H. Yakagi, 1993; O.V. Buyanov et al., 1993; V.A. Kachanov et al., 1993; M.V. Korzhik et al., 1994.) to be a promising scintillating material for precise electromagnetic calorimetry. Beam tests of electromagnetic calorimeter prototypes were performed at CERN in Autumn 1993 (V.A. Kachanov et al.) and at KEK in Winter 1994 (S. Inaba et al.). The scintillating light of the cell prototype, of size $20 \times 20 \times 180 + 200$ mm^3 (more than 20 X_0) was detected by photomultipliers (Phillips 1911 or equivalent) and the energy resolution was $\sigma E/E = 3\%/\sqrt{E} + 0.8\%$.

PWO crystals were grown by the Czochralski method in 100 mm diameter platinum crucibles in an atmosphere close to air in composition, using a mixture of W oxide and Pb oxide of 99.99% purity. These first crystals from a limited mass-production batch showed common features that suggest future technology improvements, involving the following characteristics:

1) A non-uniform light yield, from top to bottom of the crystal ingot was observed. The light yield from reference samples cut from the ingot top (seed side) was 50% higher than for samples cut from the bottom, indicating that the amount of effective scintillating centres was decreasing from the top to the bottom of the ingot.
2) The maximum of the scintillation luminescence band excited by γ-rays shifted from 490 to 455 nm from top to bottom. This reflects the contribution variation of different kinds of radiating centres to the total luminescence band intensity.
3) A different radiation hardness for top and bottom of the crystals was also observed. This phenomenon originates in the increase of point structure defects from top to bottom of the ingot.

Further modifications of PWO technology were made to improve the uniformity of the crystal properties. A model of the scintillation mechanism for PWO was developed and served to guide the improvement. The complex spectroscopic analysis of the crystal after improvement is presented here, as well as the new crystal properties achieved.

2. SCINTILLATION MECHANISM MODEL OF $PbWO_4$ CRYSTAL

2.1 *The point structure defects and crystal doping*

$PbWO_4$ crystals are sheelite type crystals. W ions are located in two types of oxygen tetrahedrons, slightly rotated in relation to each other. Each Pb ion is surrounded by eight oxygen atoms belonging to WO_4 tetrahedrons.

Analysis of data published up to now (M.V. Korzhik et al. 1994), has shown that radiating luminescence centres in $PbWO_4$ crystal are regular WO_4^{2-} centres and centres based on structure point defects in the host. The possible structure point defects (simple point approximation within a first coordination sphere) are shown in Fig. 1. In case of anion vacancy Va in crystals, two types of WO_3 defects can form according to the missing oxygen ions linking Pb and W ions or being connected only to the W ion. The local charge compensation depends on the missing oxygen ion type and can be realized in the following ways: two types of F ($Va + 2e^-$) centres; F^+ centres and recovered Pb^{1+} ions; F^+ centres and cation vacancy Vk in

the Pb ion position. The shortage of cation in W positions gives a domination of Pb^{3+} + Vk or Pb^{3+} + F^+ + Vk defects.

Thus it is to be expected that the quality of the crystal will improve significantly if grown from a melt with some tungsten overabundance, in order to favor the domination of (WO_3 + F) centres at the top of the crystal. However, the amounts of these defects decrease from top to bottom of the crystal ingot according to the abundance of W ions in the melt during the crystal growth process, while the amount of defects connected with Pb^{3+} ions increases from top to bottom of the crystal. A local compensation needs to be found to prevent the defects based on Pb^{3+} ions. This can be done by additional doping with ions of less valency — Nb^{5+} was found optimal for this purpose. For $PbWO_4$ crystals doped with Nb^{5+} in the W^{6+} ion position, significant change in structure point defect balance was found. A possible structure point defects produced by Nb^{5+} is shown in Fig. 2. Although (NbO_3 + F^+) centres will compete with (WO_3 + F) centres they will decrease the amount of structure point defects with Pb^{3+}.

2.2 *Doped and undoped crystal : spectroscopic data*

Luminescence and luminescence excitation spectra of doped by Nb and undoped samples are presented in Fig. 3.

For undoped crystals, three luminescence bands were found with excitation bands maxima at 317 nm (blue emission), 307 nm (green emission), and 322 nm overlapping a broad band of up to 350 nm (red emission). All the three bands have a strong temperature quenching at room temperature. The previous work on different kinds of tungsten crystal and on $PbWO_4$ crystals has shown that the regular WO_4^{2-} group provides blue luminescence peaked at 420 nm and green luminescence caused by centres based on WO^{3+} (M.V. Korzhik et al., 1994). The maximum of the green luminescence band shifts from 495 nm down to 481 nm when the excitation band is shifted from its longer wavelength edge (307 nm) to its shorter one (296 nm), but its shape is unchanged. This observation is in agreement with the superposition of two neighboring luminescence bands as claimed by Van Loo (1975).

The relative intensities of the green and red luminescent bands varied inversely to each other from top to bottom of an ingot, as shown in Fig. 4, for samples extracted from different positions along the ingot. These data agreed well with the structure point defects distribution elaborated above for red luminescence centres linked to the existence of Pb^{3+} ions.

However, for doped crystal with a small amount (some 10^{-5} to 10^{-4} of the mass) of Nb ions (PWO:Nb), the green luminescence intensity is slightly diminished, the red luminescence band described above as well as its excitation spectra have disappeared, while a new luminescence band with a maximum at 520 nm and an excitation of nearly 340 nm is observed. A decrease of green luminescence intensity is noted with the increase of Nb content in the crystal, while no effect is seen on blue luminescence emission. This is in agreement with our hypothesis that (NbO_3 + F^+) centres replace (WO_3 + F) centres without significantly acting on WO_4^{2-} luminescence, owing to weak energy bands overlapping.

An important peculiarity of $PbWO_4$ crystals is the increase of their photoconduction when they are excited by $\lambda < 290$ nm light, indicating an excitation into the conduction zone. For all observed luminescence bands except the 520 nm band for PWO:Nb crystals, excitation is of a maximum of about 275 nm. This maximum in reflection spectrum had been noted by R. Grasser et al., (1993) and corresponds to an allowed transition A1→ 3T1 of Pb^{2+} ions. However, the

UV luminescence of Pb^{2+} ions which exists in Pb-doped crystal or other Pb-based crystal is absent in $PbWO_4$. This facts leads us to conclude that in $PbWO_4$ crystal, scintillation is due to WO_4^{2-} luminescence as well as to structure point defect centres activated through sensitization by Pb^{2+} ions. This scheme of energy transfer processes is summarized in Fig. 5.

Owing to large Stokes shifts for luminescence bands, none of the centres have a significant energy exchange between them, and they are competitors to accept energy from Pb^{2+} ions. Because of the migration processes, WO_4^{2-} centres cannot provide a considerable contribution to total light yield. In pratice, (WO_3 + F) centres make the main contribution to the total light yield, which strongly depends on their concentration. At the present stage of the study, a direct correlation between luminescence bands of $PbWO_4$ and possible structure point defects has been established.

3. SPECTROSCOPIC AND SCINTILLATION PROPERTIES OF $PbWO_4$:Nb CRYSTALS

3.1 *Samples preparation for experimental measurements*

To study the Nb doping effect on PWO crystal properties, a set of crystals containing different Nb amounts was investigated. All full-size crystals (with length of at least 220 mm) were grown from the same crucible in the same conditions. The first crystal was grown without doping. For the other ones the Nb content expressed in mass per cent were 0.001 (N2), 0.0036 (N3), 0.0079 (N4), 0.015 (N5), 0.019 (N6), and 0.022 (N7). The reference samples for detailed investigations with dimensions $10 \times 10 \times 10$ or $20 \times 20 \times 10$ mm^3 were cut from the top of the grown ingot, and for N3 and N6 samples, pieces were cut from both the top and the bottom of the crystal. The distance between top- and bottom-cut samples from the same ingot was at least 190 mm.

3.2 *Optical spectroscopy*

The transmission spectra of N3 and N6 reference crystals are presented in Fig. 6 (a, b). The presence of Nb ions in the crystal has stabilised the transmission spectrum from top to bottom. Spectra are practicaly the same at both ends of the crystals.

In the luminescence region ($\lambda \sim 500$ nm) no effect was found on the transmission curve. However, some increase in transmission was observed in the near UV region ($\lambda \sim 350$ nm) with the increase in Nb content, displayed in Fig. 7. It indicates that Nb ions provide a change of absorption spectrum only outside the luminescence band range. In fact, Nb-doped crystals exhibit a better transmission and a lighter colouration.

The luminescence spectra excited by γ-rays are practically the same for top and bottom of the crystal doped with a small Nb amount. The luminescence spectra for the N3 sample are presented in Fig. 8 for both top and bottom. Although the Nb ions change the radiating centres' balance in the crystal, the overall luminescence spectrum shape is not affected by the increasing proportion of ($NbO_3 + F^+$) centres at the bottom of the crystal.

3.3 *Decay time measurements*

The scintillation kinetics for Nb-doped PWO crystal samples were measured by the usual start-stop method. Their decay time curves are well expressed by two exponential function approximations.

$$A1 \times \exp(-t / \tau_1) + A2 \times \exp(-t / \tau_2) + A3$$

where A3 is the noise level of random coincidences.

The main parameters τ_1 and τ_2 are presented in Table 1, where the first line refers to the undoped crystal N1 of the grown set. The decrease of τ_1 and τ_2 with sample number is attributed to the domination of the blue luminescence centres' amount, over the green luminescence (WO_3 + F) centres' amount with the increase of the Nb content in the crystal. The scintillation of crystals with a significant amount of Nb ions is mainly produced by WO_4^{2-} centres and (NbO_3 + F^+) centres with decay time constants of 2.5 ns and 12 ns, respectively.

The difference between the top and bottom samples' kinetics is small, as illustrated in Table 2, where corresponding results for samples N3 and N6 are displayed. The observed variation of decay time constants with increasing Nb content seems in good agreement with the scintillation mechanism expected from the model elaborated above.

3.4 *Light yield*

The evaluation of light yield in photoelectron/MeV was obtained by comparison of the photopeak position of the 1.2 MeV average energy γ-rays of ^{60}Co source measured by a Philips XP 2262 photomultiplier with the single electron peak of the phototube. These measurements were made for reference samples as well as for 180 mm full-length crystals. Spectra corresponding to reference sample N3 (bottom part) are shown in Fig. 9. Taking into account the values of amplification used for each spectrum, 40 photoelectrons/MeV were estimated. The effect of the Nb content on the light yield of the reference samples is summarised in Fig. 10, where the different samples are indicated on the horizontal scale refering to Nb content in mass per cent. Some improvement of light yield is observed for a 0.001–0.005% range of Nb content. It can be due to the improved transmission of Nb-doped samples below 450 nm. Nb doping provides a better uniformity of light yield along the crystal. Table 3 shows the relative position, in channels, of the photopeak of ^{60}Co source for full-size elements corresponding to N1 (undoped) and N3 samples, both 180 mm long, when the source is mounted at 1 cm (bottom) and 17 cm (top) from the photomultiplier window. The total light yield of Nb-doped crystal appears to be 13% less than for undoped crystal when the source is near the PM window. This decrease is caused by some additional influence from an absorption band at 420 nm appearing in doped crystal. Its origin needs to be further investigated. The number of photoelectron/MeV collected at the end of a 180 mm-long crystal is 12–15 due to multiple reflections and self-absorption in the bar.

4. RADIATION DAMAGE OF PWO:Nb CRYSTALS

Radiation damage of $PbWO_4$ crystals is caused by charge exchange processes in Pb^{3+} structure point defects under γ-irradiation. An additional absorption band with a maximum of around 620 nm appears for irradiated crystals with an intensity proportionnal to the absorbed dose (M.V. Korzhik et al., 1993, and G. Woody in private communications). The crystal

radiation damage near the seed (top part) is ten times less than that observed at the bottom. With compensation of recharging defects, the radiation hardness of $PbWO_4$:Nb crystals is expected to be better.

4.1 *γ-Ray Irradiation*

Reference samples N1 (undoped), N3 and N6 (top and bottom) were irradiated by a 500 R/s ^{60}Co source up to a 0.5 Mrad absorbed dose. Transmission spectra, γ-ray-excited luminescence spectra and scintillation kinetics, as well as light yield were measured after irradiation (2–4h). Transmission measurements are presented in Fig. 11 (a–e). $PbWO_4$:Nb crystals are seen as radiation-hard even with low Nb content in the crystal.

From these data one can estimate a concentration of the defects with Pb^{3+}. A compensation already exists for crystal N3 and defects concentration is estimated at less than 5×10^{17} cm^{-3}. Comparison of crystal characteristics before and after irradiation are summarised in Table 4. A good stability of PWO:Nb crystal under γ-irradiation is observed. It indicates a negligible amount of defects recharged by γ-irradiation and structure point defects that could create colour centres in the crystal.

4.2 *Electron Beam Irradiation*

The full size PWO:Nb crystal corresponding to reference sample N3 was irradiated along its longer axis with a 500 MeV electron beam at the LIL facility at CERN (J.P. Merlo et al., 1994). The impinging number of electrons corresponded to a 2 Mrad deposit at the maximum of the shower (referred to below as 2 Mrad equivalent). The effect of irradiation on crystal transmission is shown in Fig. 12 for different positions along the crystal from the top side. The homogeneity of the PWO: Nb crystal is indicated by the vicinity of the transparency curves. In Fig. 13 the transmission curves through 180 mm of the crystal before and after the electron irradiaton is displayed. The change of transparency at the emission maximum wavelength (500 nm) is less than 5%. Two months after irradiation, the crystal had returned to its original transparency. Finally, in Fig. 14 the absorption coefficient induced by irradiation is compared for an undoped crystal from a previous production batch measured in the RD18 collaboration at CERN after 0.076 Mrad irradiation by ^{60}Co γ-rays, and for a PWO:Nb crystal after 2 Mrad equivalent irradiation by the LIL electron beam. The doping with Nb further increased the good radiation hardness of normal PWO by decreasing the already small induced absorption ($\Delta K \sim 2.5$ m^{-1}) by a factor of ten ($\Delta K \sim 0.25$ m^{-1}) for Nb-doped crystal.

5. CONCLUSIONS

A model of the scintillation mechanism in $PbWO_4$ crystal was developed, compatible with the observed luminescence band mainly receiving contributions from (WO_3 + F) defects, green luminescence band centres, and WO_4^{2-} structure centres.

After a review of different structure defects, local structure defects based on Pb^{3+} ions were compensated as much as possible by Nb^{5+} ion doping.

The investigation of PWO:Nb-doped crystal properties has shown that optimal doped crystal can give a light yield 20% higher than undoped crystals and that scintillation kinetics is two-exponential with the decay time constants of 2.5 ns and 12 ns, with a negligeable third slow component.

Radiation hardness of doped crystal has been considerably improved and little change in properties was observed under Co^{60} γ-ray irradiation up to 0.5 Mrad or 500 MeV electrons up to 2 Mrad.

ACKNOWLEDGEMENTS

The authors would like to thank the INTAS foundation, which has supported part of this work, Mr J.P. Merlo for his help in gaining access to the LIL irradiation facility, and Miss E. Auffray and Mr I. Dafinei, who provided the quick-transmission measurement on the spectrometer of the RD18 collaboration after LIL irradiation.

REFERENCES

V.G. Baryshevsky, M.V. Korzhik, V.I. Moroz, V.B. Pavlenko, A.S. Lobko and A.A. Fyodorov, V.A. Kachanov and V.L. Solovjanov, B.I. Zadneprovsky, V.A. Nefyodov, P.V. Nefyodov and B.A. Dorogovin, and L.L. Nagornaja (1992), *Nucl. Instrum. Methods Phys. Res.* **A322**, pp. 231–234.

M. Kobayashi, M. Ishii, Y. Usuki, and H. Yahagi (1993), Heavy scintillators, Eds. Frontières, p. 375.

O.V. Buyanov, A.V. Dolgopolov, V.B. Gorodnichev, V.A. Kachanov, V.Yu. Khodyrev, V.A. Medvedev, V.V. Mochalov, V.A. Polyakov, Yu.D. Prokoshkin, V.V. Rykalin, P.M. Shagin, P.A. Semenov, A.V. Singovsky, V.L. Solovianov and M.N. Ukhanov, M.V. Korzhik, A.A. Fyodorov and J.P. Peigneux and M. Poulet, Beam studies of EM-calorimeter prototype built of $PbWO_4$ crystals, reported to the IV Int. Conf. on Calorimetry in High Energy, Sept. 15–19, 1993, Isola Elba, Italy.

V.A. Kachanov, Yu.D. Prokoshkin, A.V. Singovsky, V.G. Baryshevsky, M.V. Korzhik, J.P. Peigneux, M. Poulet and A.A. Fyodorov, Proceedings of IEEE'93, p. 146, Oct.-Nov. 1993, San Francisco, California, USA.

O.V. Buyanov, R. Chipaux, A.A. Fyodorov, V.A. Kachanov, V.Yu. Khodyrev, M.V. Korzhik, J.L. Faure, J.P. Peigneux, M. Poulet, Yu.D. Prokoshkin, P. Rebourgeard, V.V. Rykalin, P.M. Shagin, P.A. Semenov, A.V. Singovsky, V.L. Solovianov, LAPP-EXP 94–06 (1994), *Nucl. Instrum. Methods Phys. Res.* **A349** 62–69.

S. Inaba, M. Kobayashi, M. Nakagawa, T. Nakagawa, H. Shimizu, K. Takamatsu, T. Tsuru and Y. Yasu, KEK Preprint 94–105 (1994), submitted to *Nucl. Instrum. Methods Phys. Res.*

M.V. Korzhik, V.B. Pavlenko, T.N. Timoschenko, V.A. Kachanov, A.V. Singovsky, A.N. Annenkov, V.A. Ligun, A.A. Fyodorov, J.P. Peigneux and J.M. Moreau, LAPP-EXP 94–01 (1994), submitted to *Physica Status Solidi.*

M.V. Korzhik, V.B. Pavlenko, V.A. Katchanov, J.P. Peigneux and M. Poulet, "The scintillation mechanism in $PbWO_4$ crystals", presented at MRS'94 meeting, San Francisco, USA, April 1–8, 1994.

A.N. Annenkov, V.G. Vasiltchenko, M.V. Korzhik, *Zhurnal Pricladnoi Spectroscopii* (1994).

W. Van Loo, *Phys. Stat. Sol.* (a), **27** (1975) pp. 565–574.

W. Van Loo, *Phys. Stat. Sol.* (a), **28** (1975) pp. 225–227.

R. Grasser presented at Int. Conf. ICL'93, Aug. 9–13, 1993, Storrs, USA.

G. Woody, private communications.

J.P. Merlo, G. Métral, L. Rinolfi, N. Godinovic, I. Puljak, I. Soric, CMS TN/94–262.

FIGURE CAPTIONS

Fig. 1 The different point structure defects in $PbWO_4$ crystals.

Fig. 2 The point structure defect in $PbWO_4$:Nb crystals.

Fig. 3 The excitation: 1- λ_{lum} = 420, 2- λ_{lum} = 500, 3- λ_{lum} = 650 nm and luminescence: 4- λ_{exc} = 275, 5- λ_{exc} = 325, 6- λ_{exc} = 308, 7- λ_{exc} = 350 nm of PWO and PWO:Nb crystal: 1, 2- λ_{lum} = 420, 500, 3- λ_{lum} = 600 nm, 4- λ_{exc} = 275, 5- λ_{exc} = 307, 6- λ_{exc} = 350 nm. T = 300K.

Fig. 4 Normalized peak intensity of red and green luminescence of a $2 \times 2 \times 1$ cm^3 sample versus sample position along the ingot from top of the crystal. T = 300K.

Fig. 5 The scheme of energy transfer in $PbWO_4$ scintillators under γ-ray excitation.

Fig. 6 Optical transmission of PWO:Nb samples ($10 \times 10 \times 10$ mm^3), extracted from top and bottom of the crystal, a - N3, sample b - N6, sample T = 300K.

Fig. 7 Optical transmission of Nb-doped samples on the λ = 500 and 350 nm versus number of sample (Nb content increasing).

Fig. 8 γ-ray (^{57}Co, 122 KeV) excited luminescence of the PWO:Nb (N3) samples, extracted from the top (a) and bottom (b) of the crystal. T = 300K.

Fig. 9 Amplitude spectrum (XP2262, gain 10, shaping time 1 μs) of PWO:Nb (N3) sample ($10 \times 10 \times 10$ mm^3) with ^{60}Co (~1.2 MeV) γ source in comparison with single electron pike (gain 80, shaping time 1 μs).

Fig. 10 Light yield of Nb-doped samples ($10 \times 10 \times 10$ mm^3) versus Nb content in the melt during crystal growth.

Fig. 11 Changing of optical transmission of undoped-(a) and Nb-doped samples extracted from top (b, c) and bottom (d, e) of crystals after 5×10^5 rad absorbed dose. Measurements were done 2h after irradiation.

Fig. 12 Initial transmission (a) and transmission after 2 Mrad absorbed dose from e^- beam (b) (500 MeV) measured transversally at different positions from seed side along the growth axis.

Fig. 13 Changing of longitudinal transmission of PWO:Nb 180 mm long full-size element after 2 Mrad absorbed dose from e^- beam (500 MeV) and self recovery after 2 months, delay. T = 300K.

Fig. 14 Comparison of the effect of irradiation on undoped crystals (0.076 Mrad, ^{60}Co, 1.2 MeV) and PWO:Nb (2 Mrad, e^- beam, 500 MeV).

Table 1

Sample	τ_1 ns	τ_2 ns
1 (undoped)	3.3	19.5
2	2.9	16.5
3	2.7	13.8
4	3	13
5	3	12.8
6	2.2	11.7
7	2.3	10.4
	$\Delta\tau \approx 0.1$ ns	

Table 2

Samples	τ_1 ns	τ_2 ns
N_3 top	2.7	13.8
N_3 bottom	2.4	11.9
N_6 top	2.2	11.7
N_6 bottom	2.3	11.9

Table 3

180 mm Crystal	Top $N_{channel}$	Bottom $N_{channel}$ (near PM window)
PWO undoped	160	190
PWO:Nb (0.0038 %)	165	165

Table 4

Samples	Light yield Phe/MeV before irr.	Light yield Phe/MeV after irr.	Decay time ns τ_1 / τ_2 before irr.	Decay time ns τ_1 / τ_2 after irr.	λ_{max} nm before irr. / after irr.
N3 top	44	42	2.7 / 13.8	2.7 / 12	495 / 490
N3 bottom	40	48	2.4 / 11.9	2.4 / 11	490 / 488
N6 top	30	30	2.2 / 11.7	2.5 / 12.3	490 / 490
N6 bottom	25	25	2.3 / 11.9	2.5 / 11	488 / 488

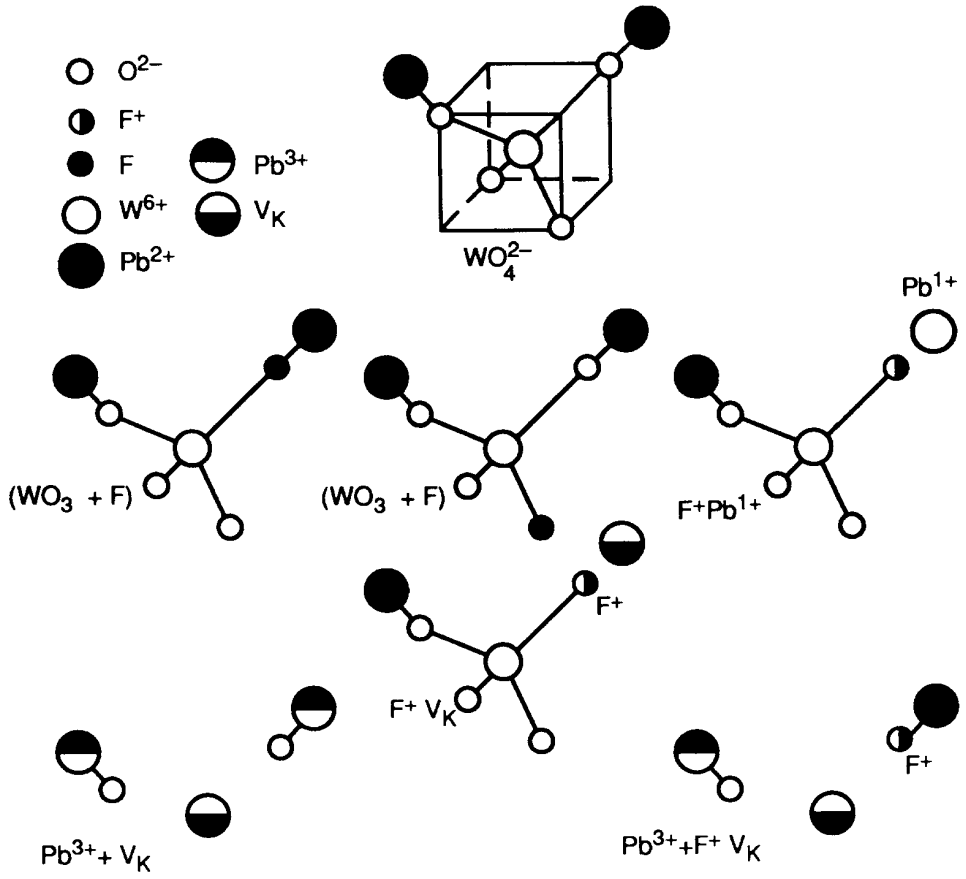

Fig. 1

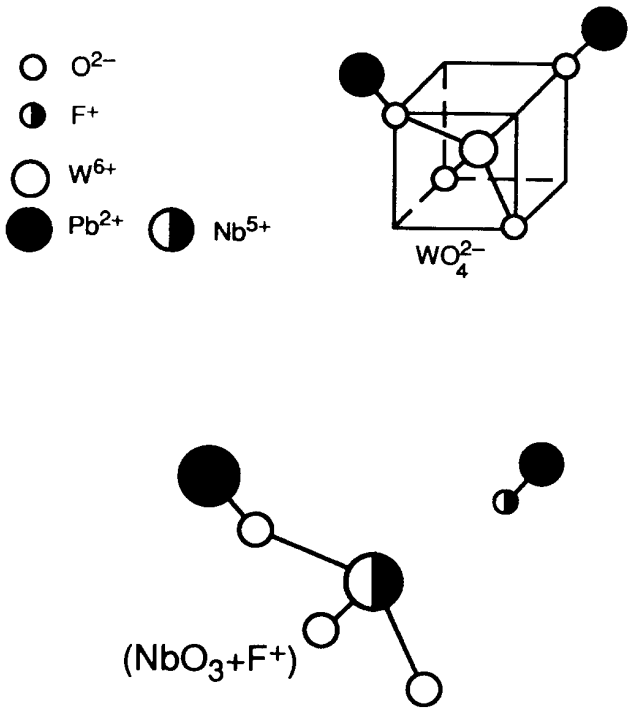

Fig. 2

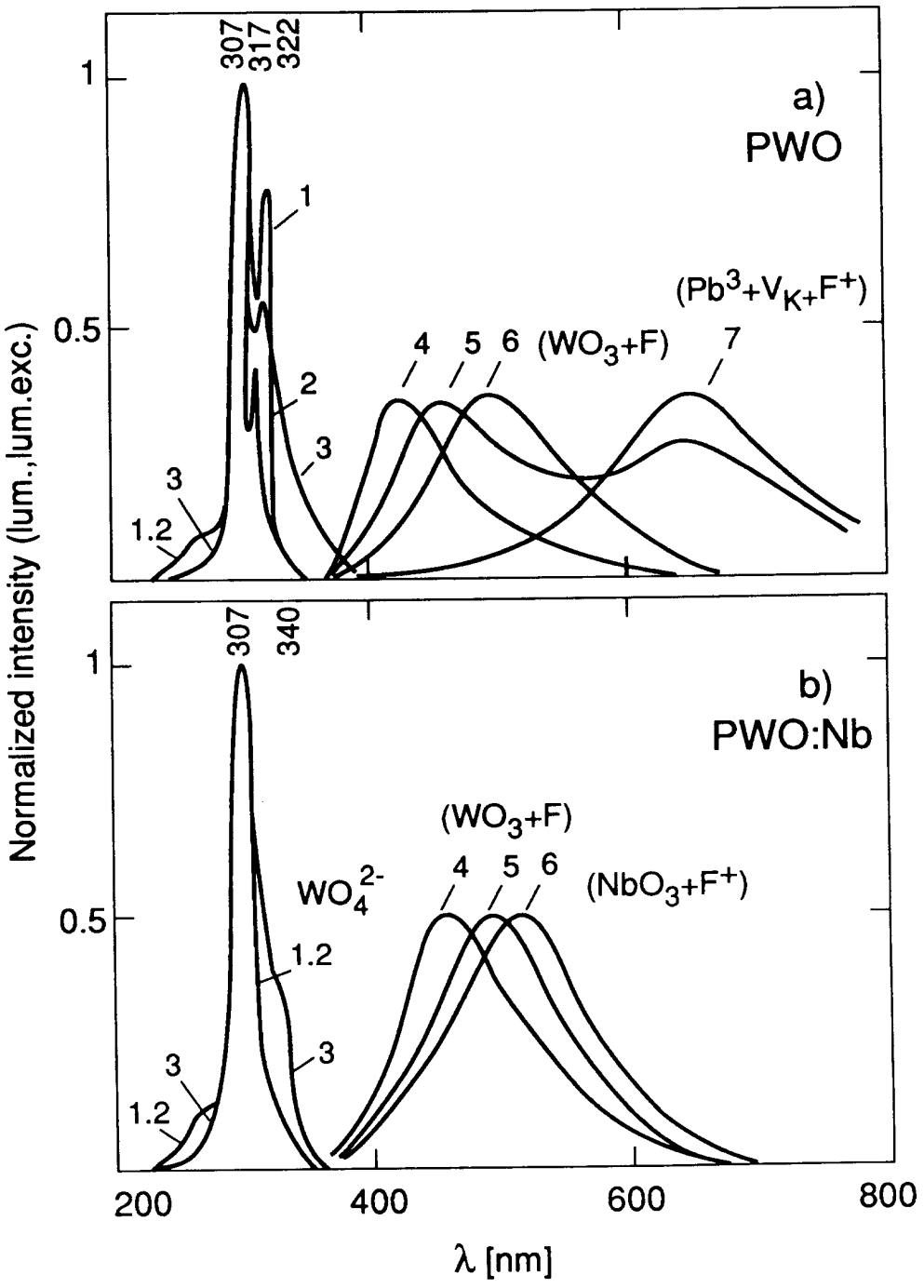
Normalized intensity (lum.,lum.exc.)
1
0.5
307
317
322
a)
PWO
1
2
3
3
1.2
(Pb3+VK+F+)
4
5
6
(WO3+F)
7
1
0.5
307
340
b)
PWO:Nb
(WO3+F)
WO4 2-
4
5
6
(NbO3+F+)
1.2
3
3
1.2
200
400
600
800
λ [nm]

Fig. 3

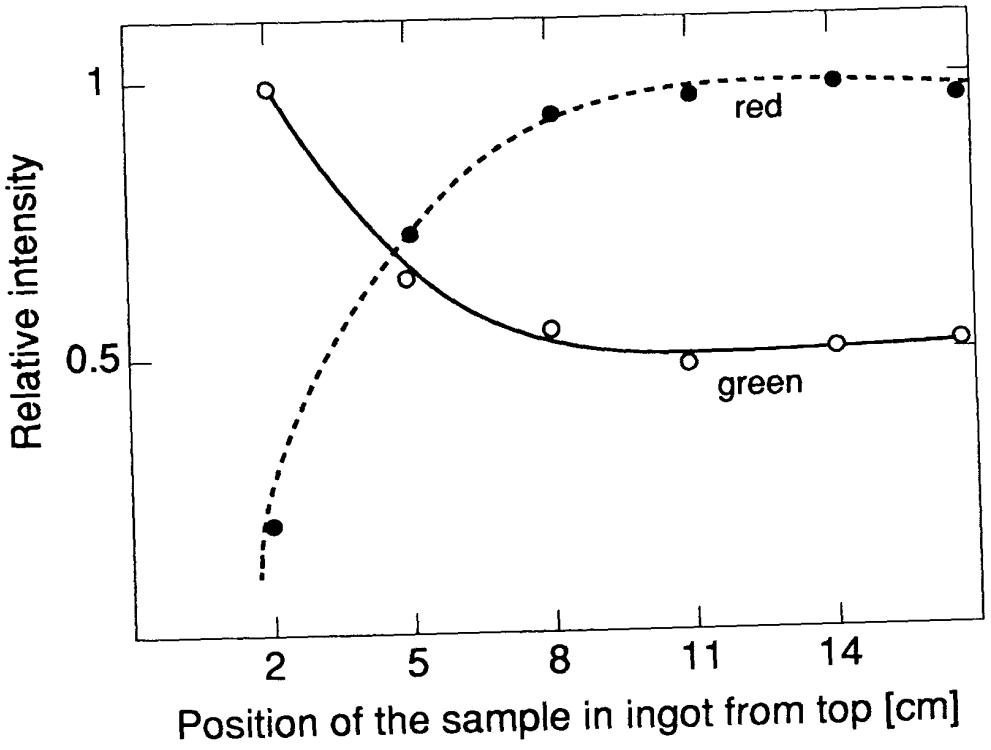
Relative intensity
1
0.5
red
green
2
5
8
11
14
Position of the sample in ingot from top [cm]

Fig. 4

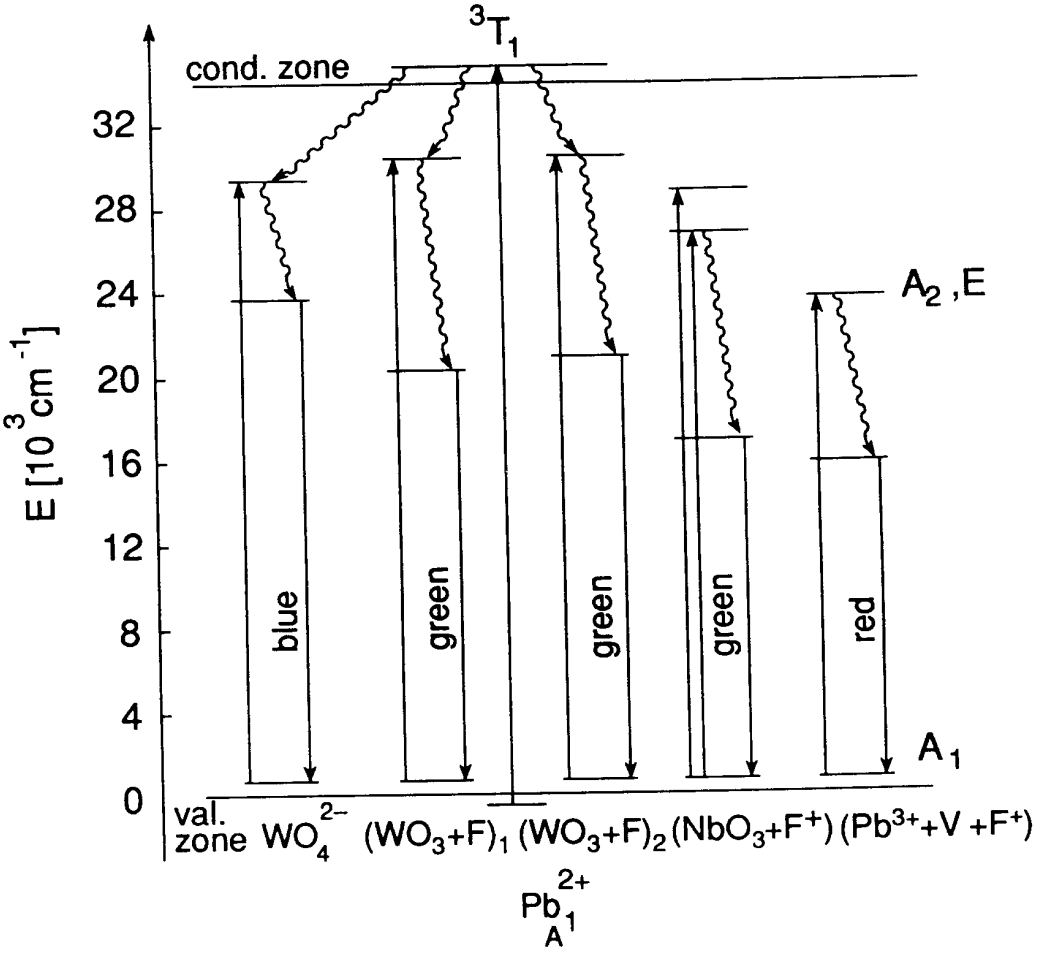
$^3T_1$
cond. zone
32
28
24
20
16
12
8
4
0
E [10^{3}cm^{-1}]
blue
green
green
green
red
A_2 ,E
A_1
val. zone
WO_4^{2-}
$(WO_3+F)_1$
$(WO_3+F)_2$
(NbO_3+F^+)
$(Pb^{3+}+V+F^+)$
$Pb^{2+}_{A_1}$

Fig. 5

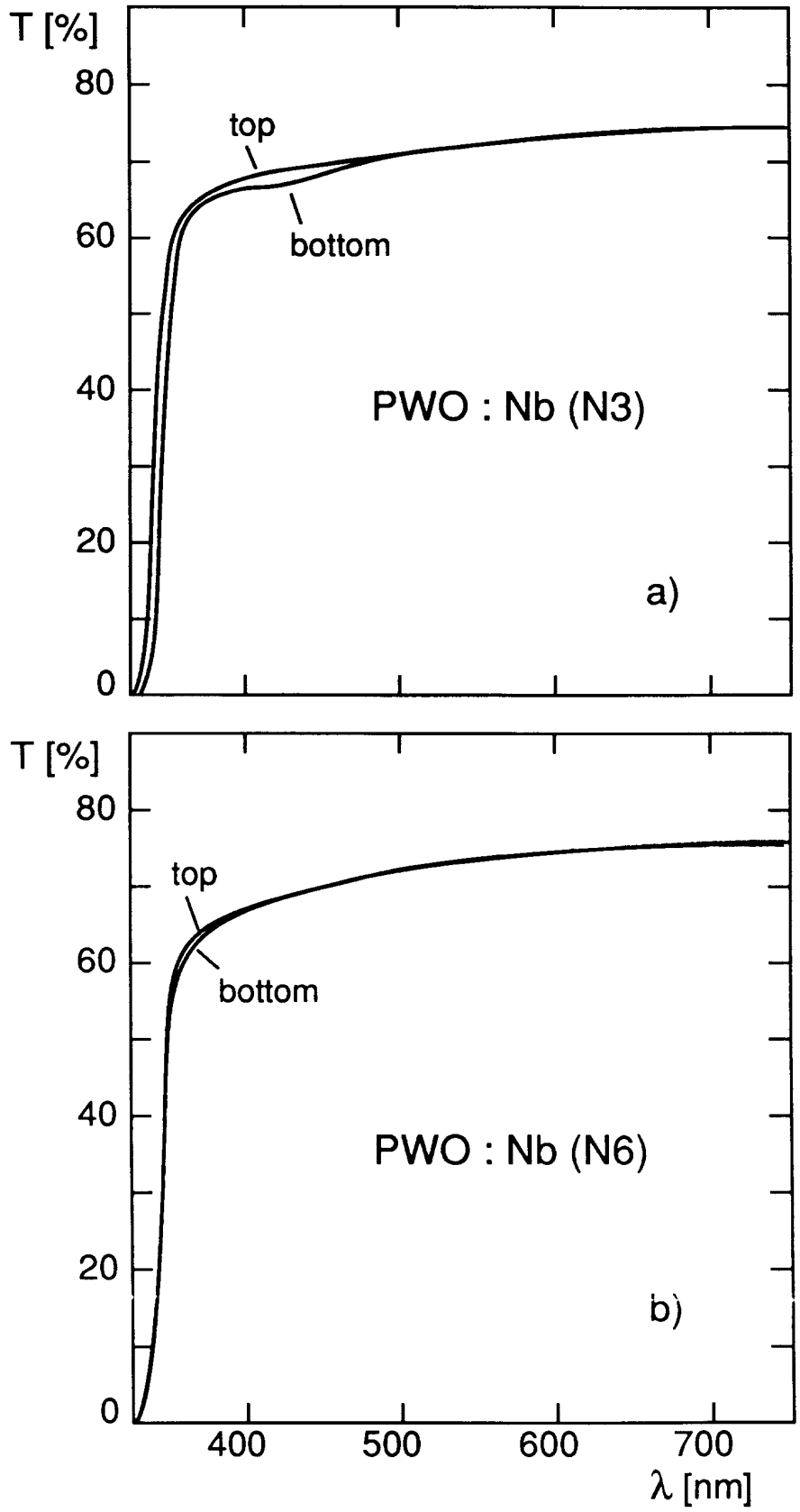
T [%]
80
60
40
20
0
top
bottom
PWO : Nb (N3)
a)
T [%]
80
60
40
20
0
top
bottom
PWO : Nb (N6)
b)
400
500
600
700
λ [nm]

Fig. 6

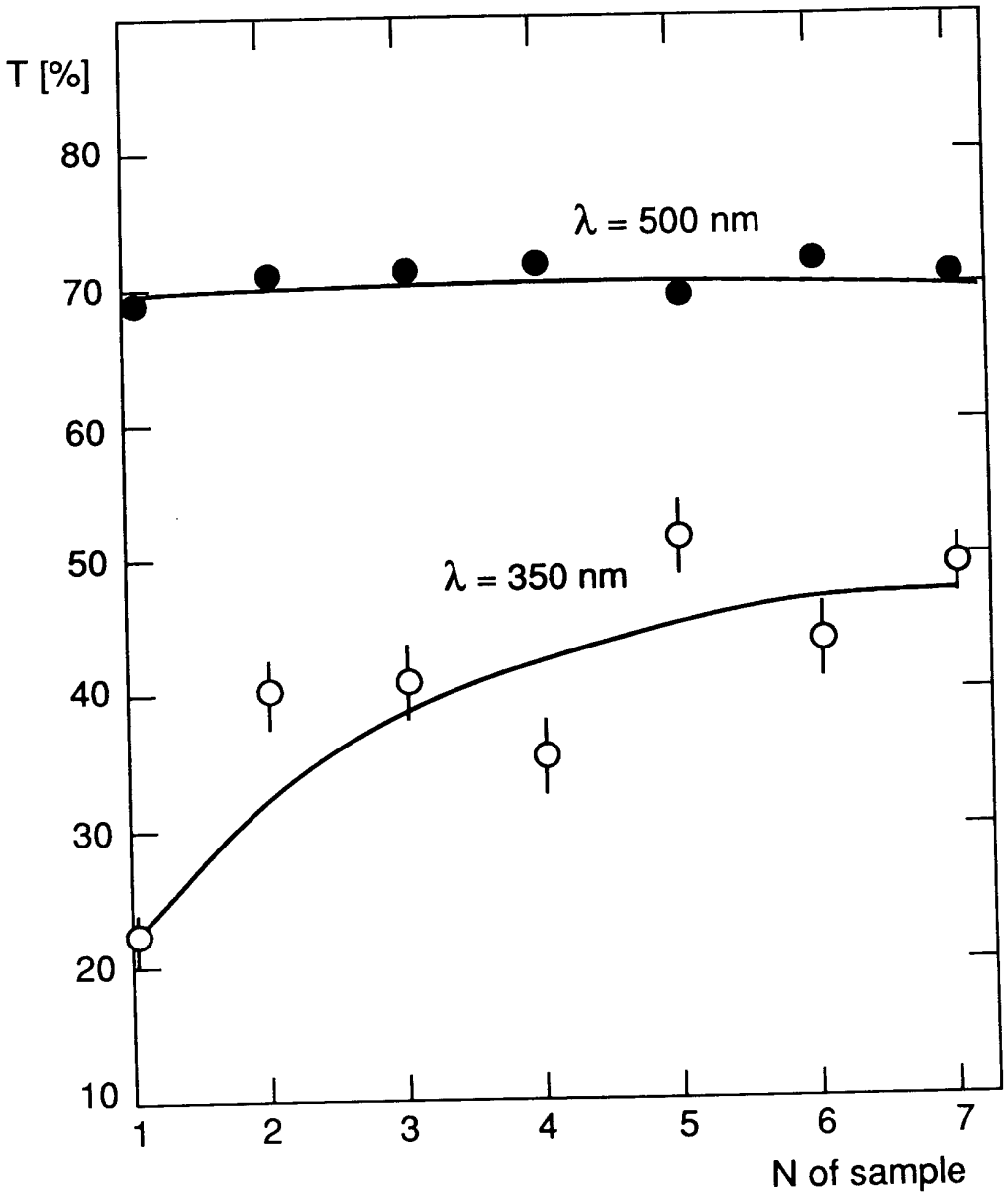

Fig. 7

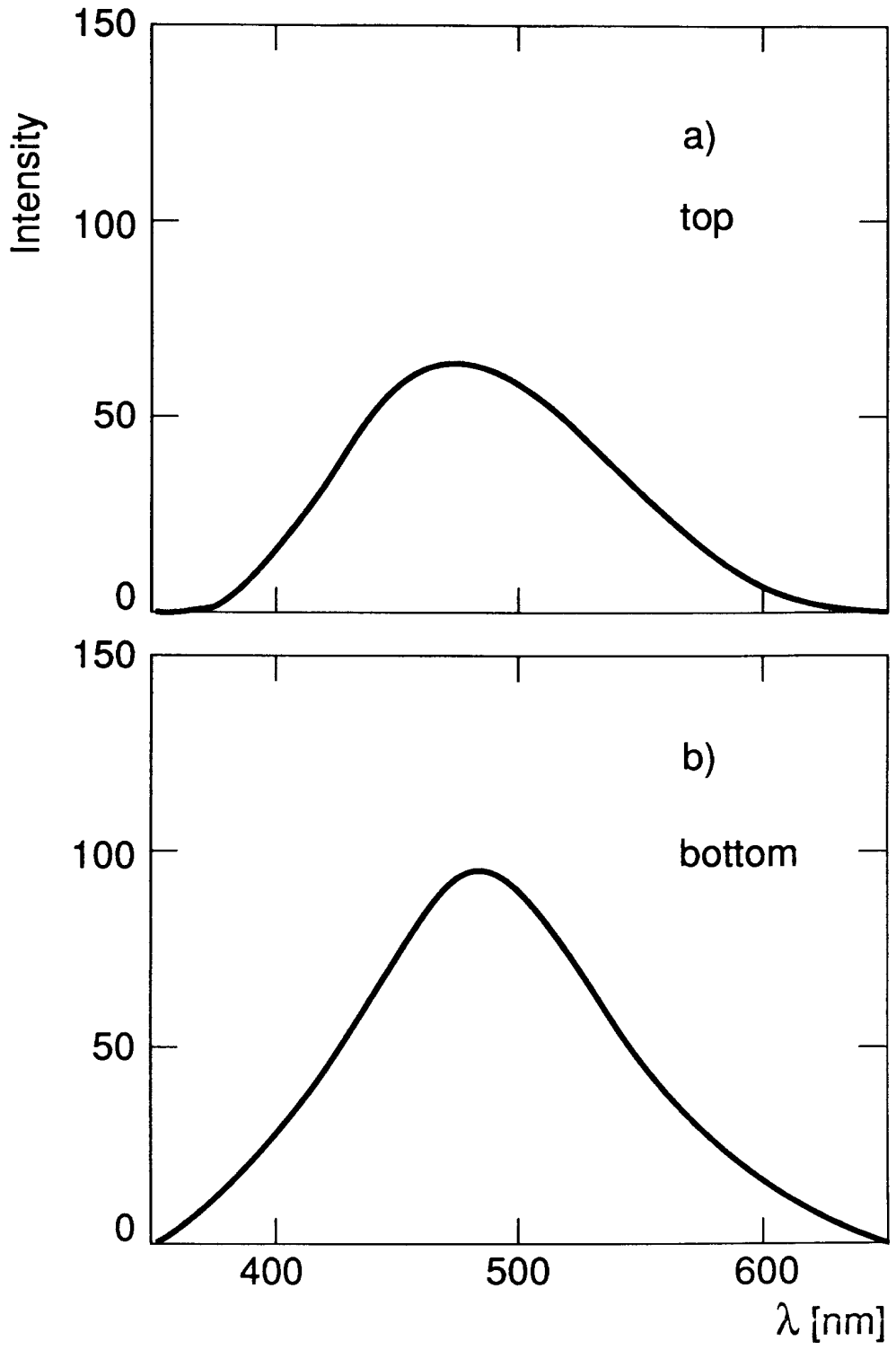
150
100
50
0
Intensity
a)
top
150
100
50
0
b)
bottom
400
500
600
λ [nm]

Fig. 8

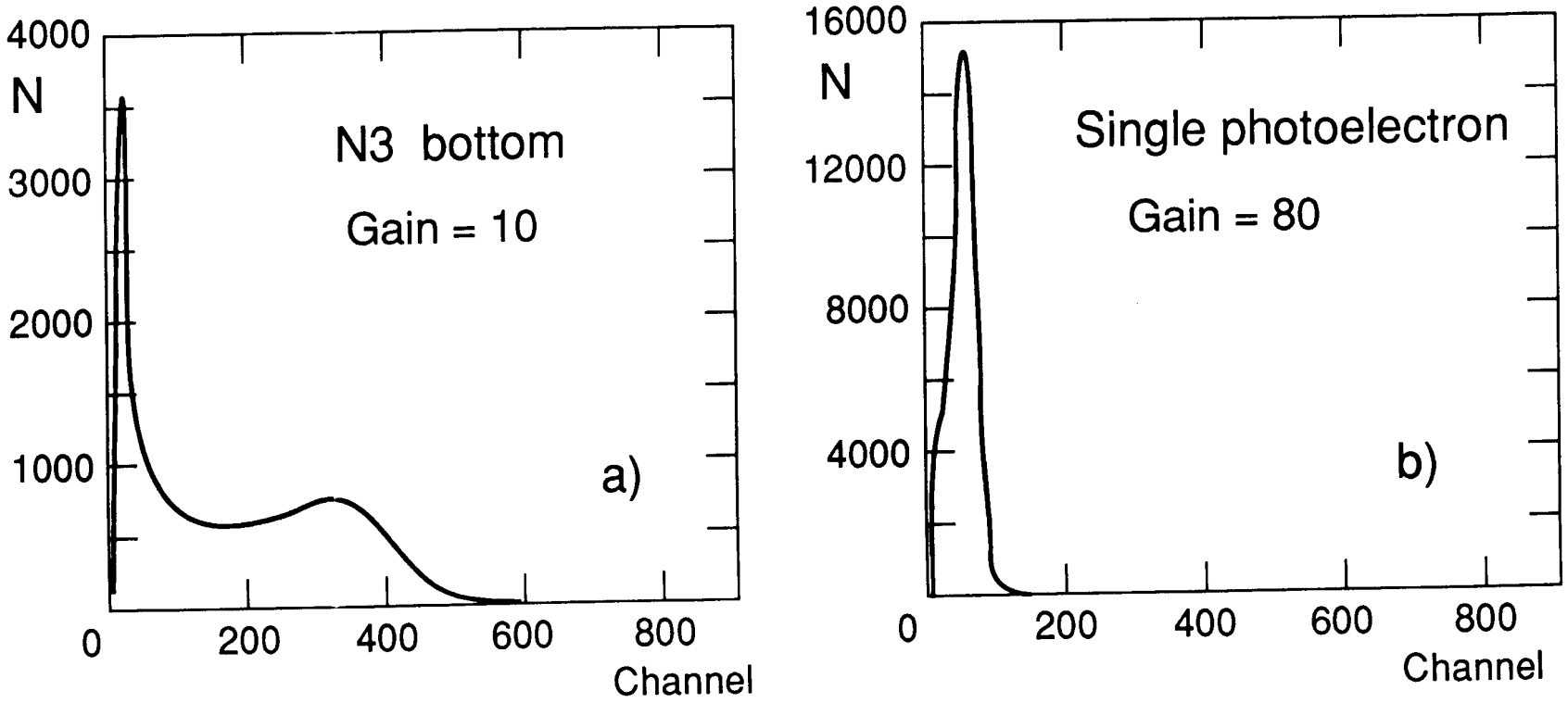
4000
N
3000
2000
1000
N3 bottom
Gain = 10
a)
0
200
400
600
800
Channel
16000
N
12000
8000
4000
Single photoelectron
Gain = 80
b)
0
200
400
600
800
Channel

Fig. 9

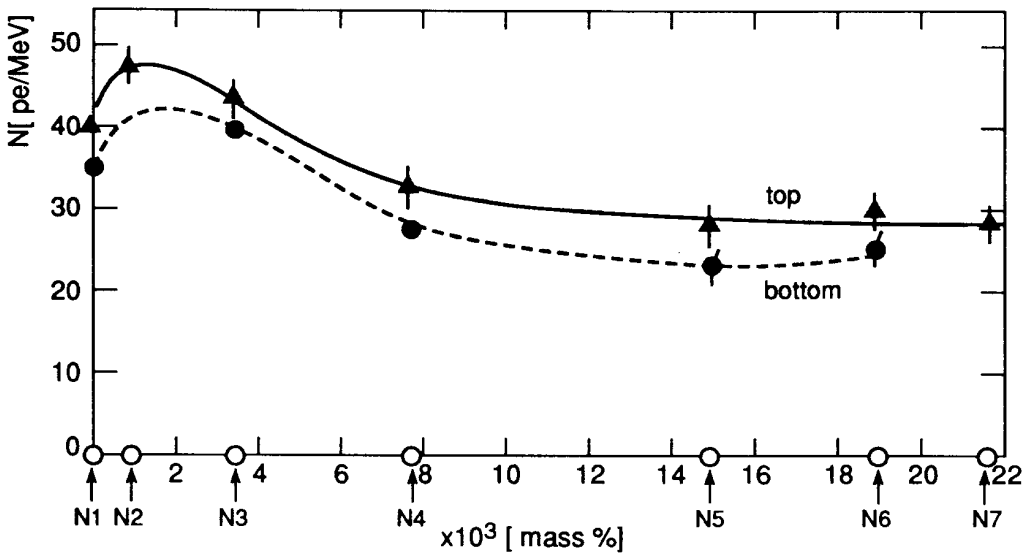
N[pe/MeV]
50
40
30
20
10
0
top
bottom
2
4
6
8
10
12
14
16
18
20
22
N1
N2
N3
N4
N5
N6
N7
x10^3 [mass %]

Fig. 10

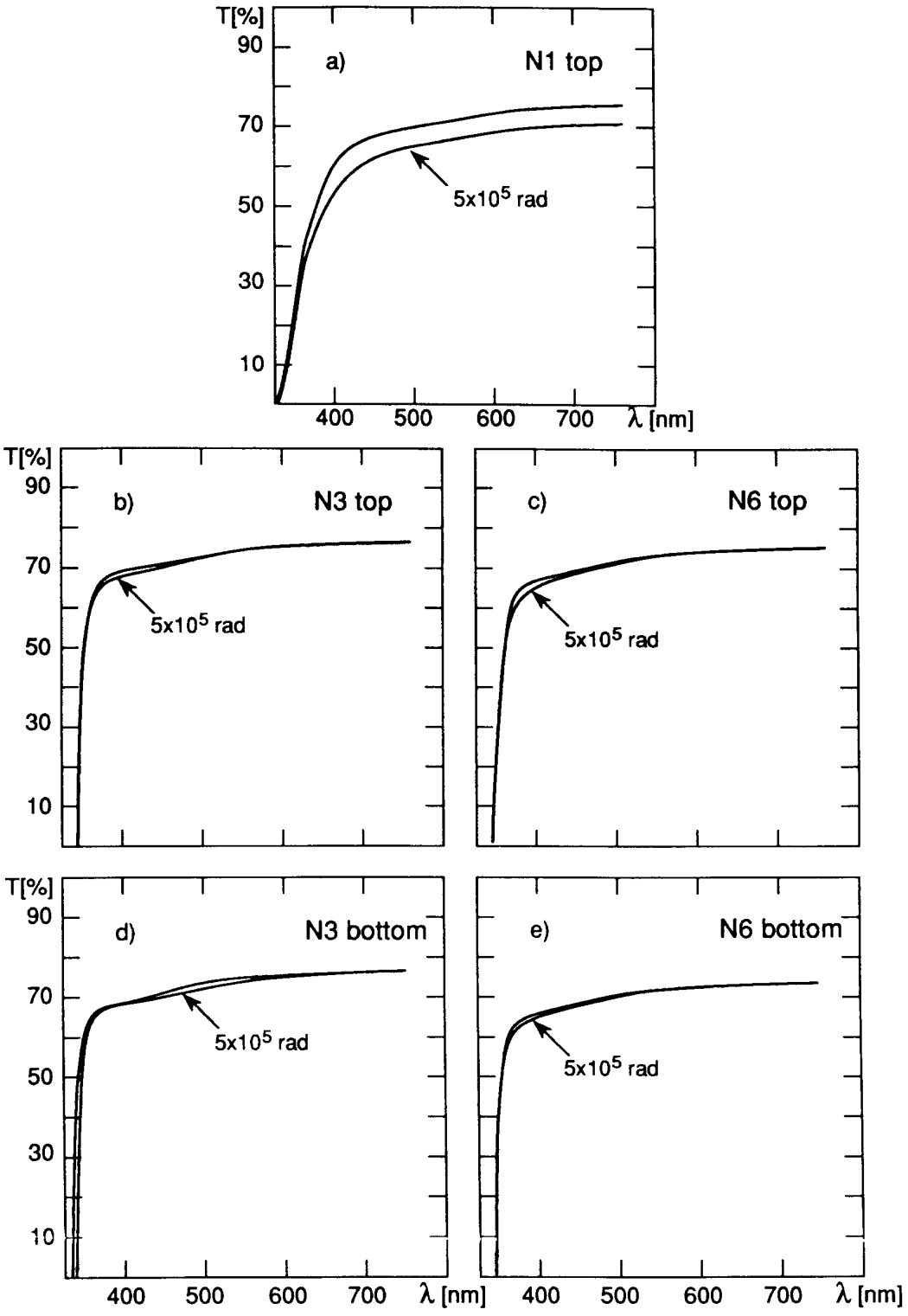
T[%]
90
70
50
30
10
a)
N1 top
5x10^5 rad
400
500
600
700
λ [nm]
b)
N3 top
c)
N6 top
d)
N3 bottom
e)
N6 bottom

Fig. 11

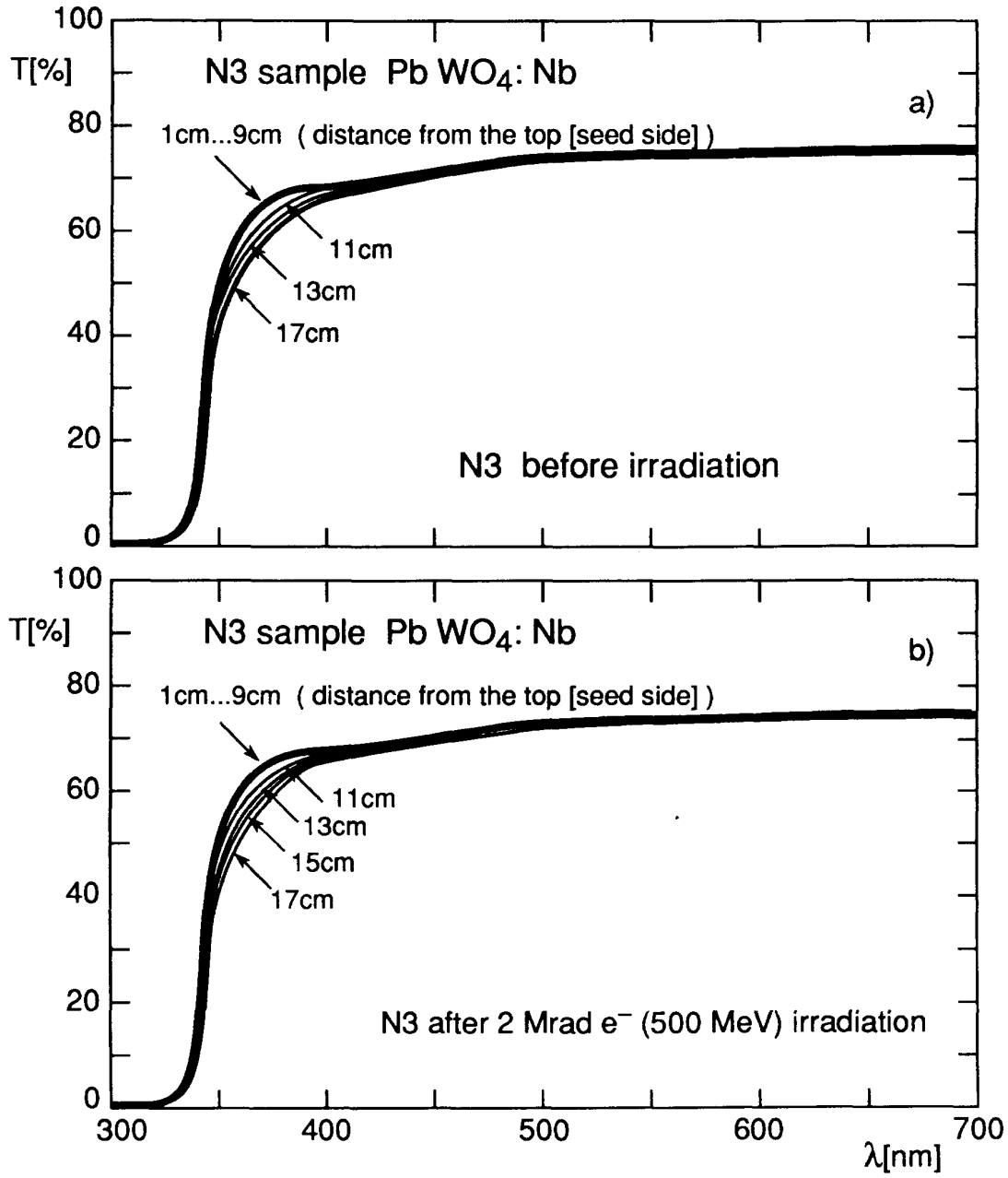
100
T[%]
80
60
40
20
0
N3 sample Pb WO4: Nb
a)
1cm...9cm (distance from the top [seed side])
11cm
13cm
17cm
N3 before irradiation
100
T[%]
80
60
40
20
0
N3 sample Pb WO4: Nb
b)
1cm...9cm (distance from the top [seed side])
11cm
13cm
15cm
17cm
N3 after 2 Mrad e⁻ (500 MeV) irradiation
300
400
500
600
700
λ[nm]

Fig. 12

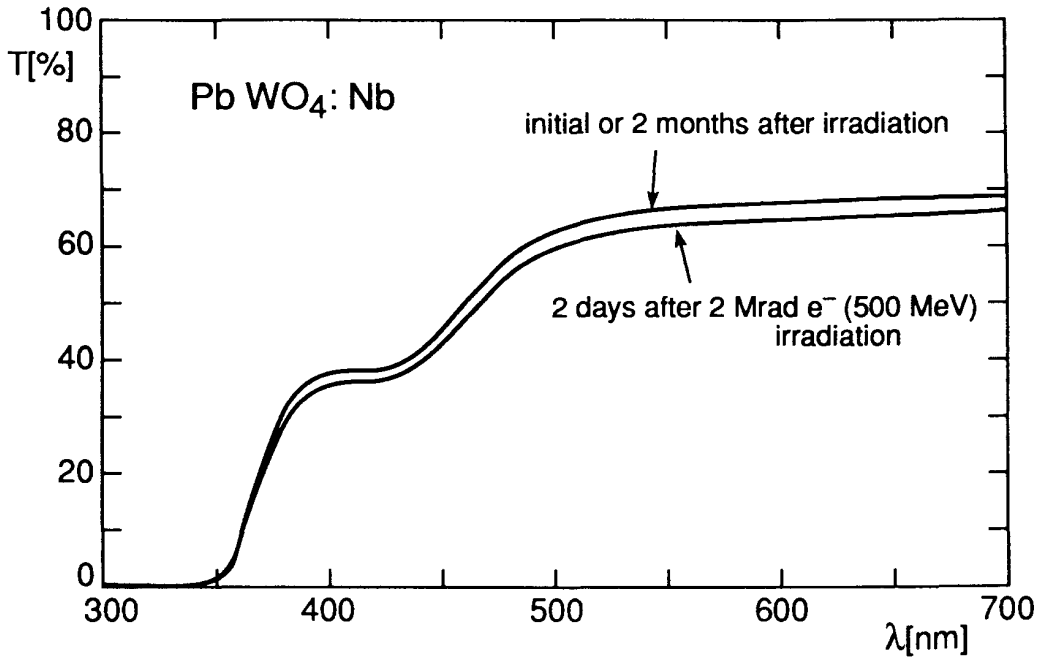
100
T[%]
80
60
40
20
0
Pb WO4: Nb
initial or 2 months after irradiation
2 days after 2 Mrad e⁻ (500 MeV)
irradiation
300
400
500
600
700
λ[nm]

Fig. 13

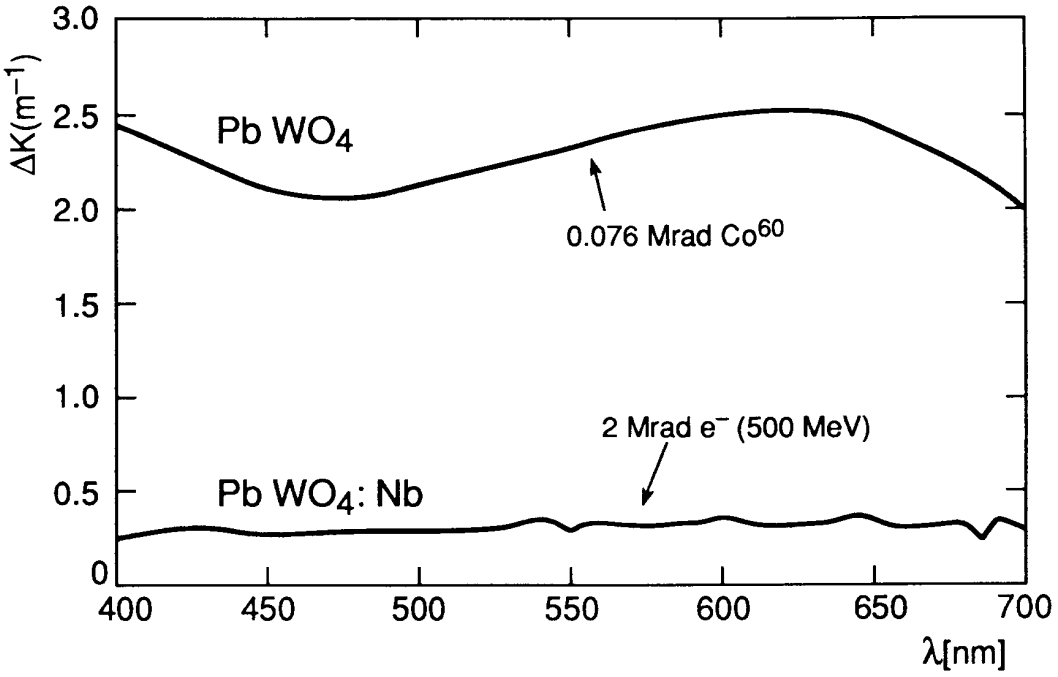
3.0
2.5
2.0
1.5
1.0
0.5
0
ΔK(m⁻¹)
Pb WO4
0.076 Mrad Co60
2 Mrad e⁻ (500 MeV)
Pb WO4: Nb
400
450
500
550
600
650
700
λ[nm]

Fig. 14